JACS JOURNAL OF THE AMERICAN CHEMICAL SOCIETY

Caltech Library

Subscriber access provided by Caltech Library

Communication

Lewis Acid Enhancement of Proton Induced CO Cleavage: Bond Weakening and Ligand Residence Time Effects

Joshua A. Buss, David G. VanderVelde, and Theodor Agapie

J. Am. Chem. Soc., **Just Accepted Manuscript** • DOI: 10.1021/jacs.8b05874 • Publication Date (Web): 23 Jul 2018

Lewis Acid Enhancement of Proton Induced CO_2 Cleavage: Bond Weakening and Ligand Residence Time Effects

Joshua A. Buss, David G. VanderVelde, and Theodor Agapie

Division of Chemistry and Chemical Engineering, California Institute of Technology, 1200 E. California Blvd. MC 127-72, Pasadena, CA, USA

Supporting Information Placeholder

ABSTRACT: Though Lewis acids (LAs) have been shown to have profound effects on carbon dioxide (CO_2) reduction catalysis, the underlying cause of the improved reactivity remains unclear. Herein, we report a well-defined molecular system for probing the role of LA additives in the reduction of CO_2 to carbon monoxide (CO) and water. Mo(0) CO_2 complex (**2**) forms adducts with a series of LAs, demonstrating CO_2 activation that correlates linearly with the strength of the LA. Protons induce C–O cleavage of these LA adducts, in contrast to the CO_2 displacement primarily observed in the absence of LA. CO_2 cleavage shows dependence on both bond activation and the residence time of the bound small molecule, demonstrating the influence of both kinetic and thermodynamic factors on promoting productive CO_2 reduction chemistry.

As the terminal product of fossil fuel combustion, the conversion of carbon dioxide (CO_2) to energy-dense, liquid fuels is a necessary step in closing an anthropogenic carbon cycle.[1] Technologies for the capture,[2] copolymerization,[3] and hydrogenation[4] of CO_2 have recently emerged, and their study and design is topical. However, the controlled reduction of CO_2 with protons and electrons is most relevant to artificial photosynthesis and couples most directly to the storage of renewable energy in chemical bonds.[1d,5] Due to the kinetic stability of CO_2,[6] the range of products formed in a narrow potential window, and competing reduction reactions,[5b,8] efficient and robust catalysts capable of the selective reduction of CO_2 remain a subject of significant interest.[6a]

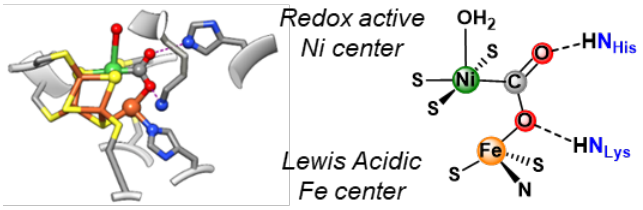

Figure 1. Solid-state structure (left, PDB: 4UDX)[7] and schematic representation (right) of the CO_2-bound NiFe-CODH active site.

In nature, the two-electron two-proton reduction of CO_2 is executed reversibly by CO-Dehydrogenases (CODH).[9] The enzyme active site of NiFe CODH features a redox active Ni center and an Fe(III) ion that coordinate CO_2 in a μ-ηC:ηO binding motif (Figure 1).[9b] Added Lewis acids (LAs) promote rate enhancements and redox potential shifts in electrocatalytic CO_2 reduction.[10] This strategy of cooperative CO_2 activation has inspired molecular mimics in the form of ligand scaffolds that feature LAs in the coordination sphere,[11] heterobimetallic complexes,[12] exogenous LA addition to CO_2 bound metal complexes or CO_2 reduction intermediates,[9a,13] and reduction catalysis combining transition metals and diboranes.[14] Though LAs are capable of promoting CO_2 binding[9a] and increasing the degree of CO_2 activation,[13c] systematic investigations of their effect on reactivity of the bound CO_2 unit remain scant. Herein, we describe a study correlating Lewis acidity and the degree of CO_2 activation in a low-valent Mo complex.[15] Moreover, we demonstrate that LA addition facilitates C–O bond cleavage, chemistry that does not proceed from the parent LA-free CO_2 complex, via *both* kinetic stabilization and increased small molecule activation.

Dinitrogen adduct **1** reversibly binds CO_2, resulting in formation of an η^2-CO_2 complex, **2** (Scheme 1). Under an atmosphere of $^{13}CO_2$, the $^{31}P\{^1H\}$ and $^{13}C\{^1H\}$ NMR spectra display a coupling doublet and triplet at 62.8 and 192.4 ppm (^2J(C,P) = 29.3 Hz), respectively, consistent with coordination of a single $^{13}CO_2$ molecule.[16] The IR spectrum of **2** displays stretches at 1716 and 1198 cm^{-1}, sensitive to $^{12}C/^{13}C$ isotopic labeling, again supporting a bound CO_2 motif.[16-17] Solid-state analysis of single crystals of **2** grown under a CO_2 atmosphere confirm the η^2 binding mode (Figure 2).

Interested in the thermodynamics of this reversible small molecule binding, longitudinal relaxation (T_1) times were measured for the relevant ^{13}C and ^{15}N resonances of an equilibrium mixture of **1-^{15}N**, **2-^{13}C**, $^{15}N_2$ and $^{13}CO_2$. Uncharacteristically short values

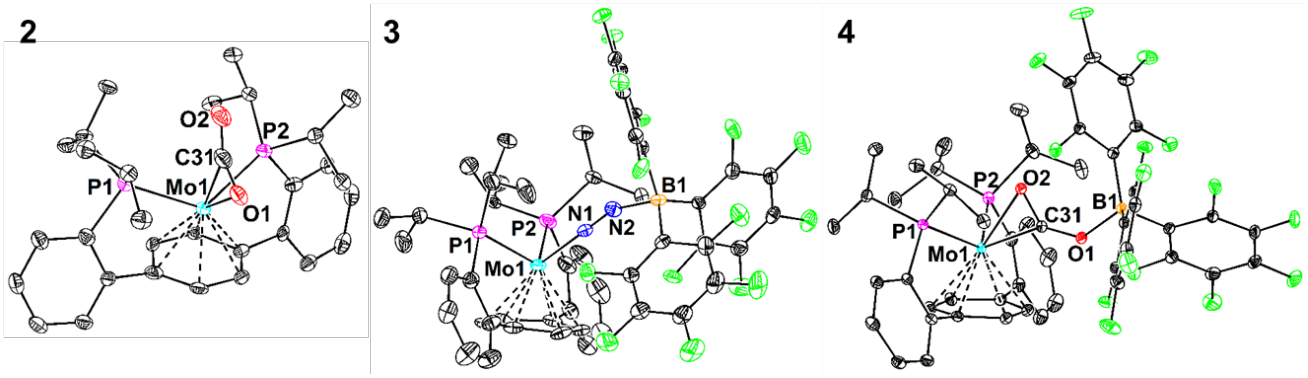

Figure 2. Solid-state structures of complexes **2**-**4**. Thermal anisotropic displacement ellipsoids are shown at the 50% probability level. H-atoms are omitted for clarity. Selected bond distances [Å] and angles [°]—**3**: Mo1–N1 1.913(2), N1–N2 1.163(3), N2–B1 1.585(37), ∠Mo1-N1-N2 179.1(3), ∠N1-N2-B1 158.2(1.2); **4**: Mo1–O2 2.2535(6), Mo1–C31 2.0574(8), O2–C31 1.246(1), C31–O1 1.275(1), O1–B1 1.554(1), ∠O2-C31-O1 130.93(8), ∠C31-O1-B1 132.13(7).

Scheme 1. CO_2 binding and LA adduct formation at low-valent Mo.[‡]

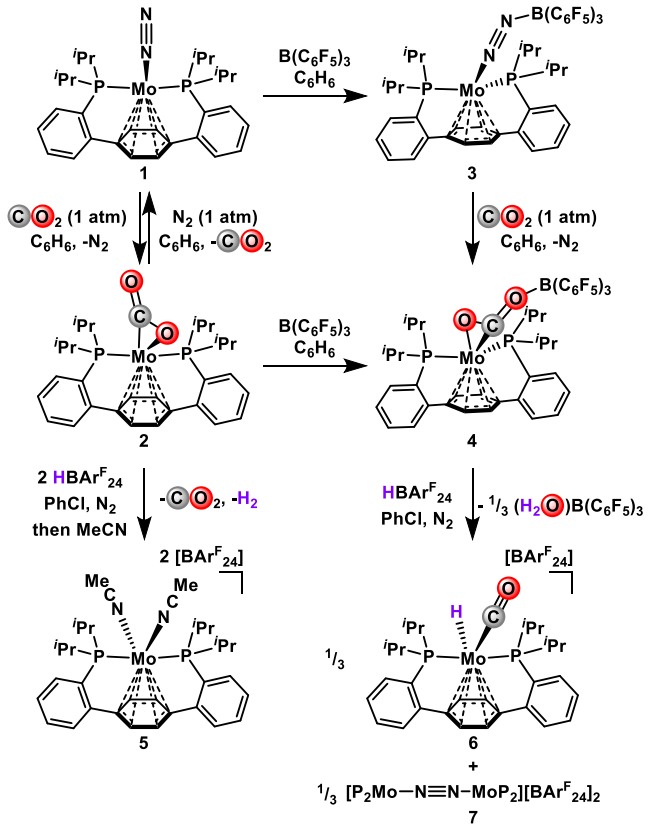

[‡]$HBAr^{F}_{24}$ = $[H(Et_2O)_2][BAr^{F}_{24}]$ (BAr^{F}_{24} = tetrakis[3,5-bis(trifluoromethyl)phenyl]borate)

were observed for **1**-^{15}**N**, free $^{15}N_2$, **2**-^{13}**C**, and free $^{13}CO_2$—5.1(4), 4.9(3), 12.5(4), and 16.8(7) s, respectively.[18] These short and near equivalent T_1 times suggest an exchange process that enables new relaxation pathways unavailable to the free small molecules.[19] In the case of CO_2, exchange was confirmed by magnetization transfer. The high lability of the CO_2 ligand was reflected in the reactivity of **2**. Addition of excess acid to **2** at room temperature resulted in CO_2 dissociation and formation of Mo(II) dication **5** (Scheme 1), via a Mo hydride cation,[20] which has been observed in stoichiometric reactions with acid. In CO_2 reduction electrocatalysis, conversion to the metal hydride moves selectivity away from CO, affording either formate or H_2, and representing a branching point in terms of defining the selectivity of CO_2 reduction.[21]

Despite its implication as a critical step in CO_2 to CO reduction catalysis,[22] there is a paucity of reports of the protonation of well-defined CO_2 adducts of transition metals.[13a,23] Indeed, protolytic dissociation and subsequent gas analysis was a common characterization technique for metal-CO_2 complexes.[24]

Borane LAs have been employed to activate metal coordinated small molecules.[13a,13c,25] Addition of the strong LA tris(pentafluorophenyl)borane ($B(C_6F_5)_3$) to complex **1** affords the LA/base adduct **3** (Scheme 1), as confirmed by XRD (Figure 2). The bond metrics of complex **3** are consistent with significant activation of the N_2 unit.[26] The solid-state IR spectrum corroborates weakening of the N–N bond, with the stretch red shifting by 134 cm^{-1}. NMR spectroscopy supports a strong borane/nitrogen interaction in solution, with both the ^{19}F (-135.0, -157.9, and –166.8 ppm)[27] and ^{11}B (-14.4 ppm)[28] spectra consistent with four-coordinate boron.

Treating **3** with CO_2, or **2** with $B(C_6F_5)_3$, results in the formation of a new LA adduct, **4**, quantitatively. Contrasting the equilibrium between complexes **1** and **2**, which slightly favors N_2 binding (K_{eq} = 0.48), addition of $B(C_6F_5)_3$ renders CO_2 binding irreversible (Scheme 1), likely a consequence of the strong B–O interaction; **4** is stable under N_2 in both the solid-state and solution. The triplet for the $^{13}CO_2$ unit of isotopically labeled **4**-^{13}**C** moves downfield relative to **2** (218.9 ppm, C_6D_6) and exhibits smaller ^2J(C,P) scalar coupling (11.47 Hz). Akin to **3**, the ^{11}B and ^{19}F NMR data are consistent with four-coordinate boron.

The solid-state structure of **4** exhibits a μ-η^{2}C,O:ηO bridging CO_2 unit between Mo and B (Figure 2). Borane binding to metal-coordinated CO_2 is rare,[13c] but **4** displays similar bond metrics to such complexes. The structural parameters are consistent with significant CO_2 activation, a phenomenon also borne out in the IR spectrum. The stretches for the CO_2 unit shift to 1602 cm^{-1} and 1218 cm^{-1}, as confirmed by isotopic labeling.

When stabilized with a LA, the reactivity of the Mo CO_2 complexes is decidedly different. The reaction of **4**-^{13}**C** with $HBAr^{F}_{24}$ results in the formation of a single diamagnetic Mo complex (Scheme 1). The ^{31}P{^{1}H} and ^{13}C{^{1}H} NMR spectra display a doublet (92.64 ppm) and triplet (220.08 ppm), respectively (^2J(P,C) = 14.6 Hz), consistent with CO_2 cleavage to a metal-bound carbonyl. The identity of this product was confirmed as carbonyl hydride cation, **6**-^{13}**C**, via XRD and independent synthesis.[29]

A balanced reaction for the formation of **6** requires a reductant. When run under N_2, the electrons are provided by **1**, which is generated under the reaction conditions upon borane displacement. Concomitantly with generation of **6**, a paramagnetic Mo(I)–N_2–Mo(I) dinuclear complex,

7, is formed, as confirmed by XRD. Quantifying conversion to **6** shows *ca.* 33% C–O cleavage, consistent with a process involving **1** acting as a single electron reductant; one electron oxidation of **1** with [Fc][BAr^F_{24}] likewise provides **7**. Borane speciation in the protonation reactions was tracked by ^{19}F NMR spectroscopy, supporting formation of a bis(borane) hydroxide[30] and subsequent protonation to a borane aquo adduct.[31] Remarkably, LA coordination "turns on" C–O cleavage chemistry, affording CO and H_2O from CO_2 and acid. Borane binding facilitates the delocalization of electron density from the low-valent Mo center into the LUMO of CO_2, in a push-pull mechanism, similar to the "bifunctional attack" proposed for NiFe-CODH.[7]

Figure 3. CO_2 Activation as a function of Lewis Acidity.[‡]

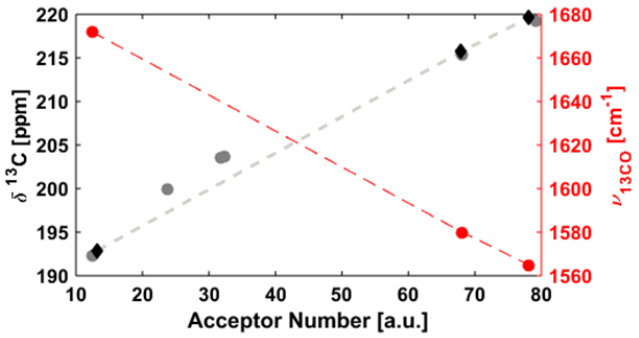

[‡]The ^{13}C chemical shift of the CO_2 ligand, in PhCl (♦) and PhCl/Et_2O (●), tracks inversely with the C–O stretching frequency (●).

Interested in the generality of the CO_2 activation observed upon LA coordination to **2**, a series of alkali metal (Na(BAr^F_{24}) and Cs(BAr^F_{24})) and borane ($B(C_6H_2F_3)_3$, $B(C_6F_5)_3$, and $B(C_6H_3(CF_3)_2)_3$) LAs were added to **2-^{13}C**. In each case, $^{13}C\{^1H\}$ and $^{31}P\{^1H\}$ NMR spectroscopies supported adduct formation, displaying resonances shifted downfield and upfield, respectively, from those of **2** (Tables 1 and S2). The degree of CO_2 activation, as reported by the ^{13}C chemical shift, trends linearly with the strength of the LA, as quantified by the acceptor number (AN, Figure 3).[32] A similar linear trend is seen when comparing AN vs. ν_{CO2},[33] suggesting that, in this case, the ^{13}C chemical shift of the bound CO_2 ligand correlates with the degree of C–O bond activation.

Revisiting protonation with these new LA adducts (Scheme 2),[34] we were gratified to see that in all cases, C–O bond cleavage was enhanced (Table 1). The extent of C–O cleavage[35] in PhCl/Et_2O[36] increased to roughly the same level, in the rage of 4-9%, and not proportionally with the LA AN. Changing to neat PhCl resulted in a further increase to bond cleavage up to 13-16%. Importantly, a two-fold increase in formation of **6-^{13}C** is observed for $B(C_6H_2F_3)_3$ and $B(C_6F_5)_3$ adducts of **2-^{13}C**, despite little perturbation in their respective ^{13}C NMR chemical shifts between the two solvent systems. These data are inconsistent

Scheme 2. Protonation of *in situ* formed LA adducts.

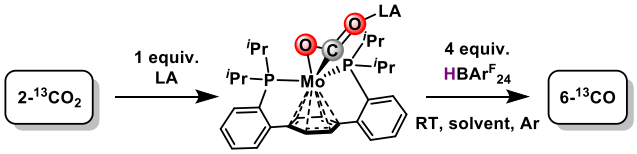

Table 1: CO_2 Activation, Exchange Rate, and Cleavage Data

	LA	AN	δ ^{13}C (ppm)	Rate x 10^{-6} (s^{-1})	% CO Cleavage	
					Abs[a]	Rel[b]
PhCl/Et_2O	None	12.4	192.3	>200[c]	0	0
	Cs(BAr^F_{24})	23.7	199.9	20	7	21
	Na(BAr^F_{24})	31.8	203.5	6	4	12
	Na(BAr^F_{24})[d]	32.4	203.7	2	5	15
	$B(C_6H_2F_3)_3$	68.1	215.3	5	4	12
	$B(C_6F_5)_3$	79.2	219.3	9	9	18
PhCl	None	13.2	192.9	>200[c]	1	3
				>70[e]	10[f]	30[f]
	$B(C_6H_2F_3)_3$	67.9	215.7	2	13	39
	$B(C_6F_5)_3$	78.1	219.6	2	17	51
					33[g]	99[g]
	$B(C_6H_3(CF_3)_2)_3$	82.7	219.1	1	16	48

[a]Determined by relative integration (^{31}P NMR spectroscopy) against a Ph_3P=O internal standard. [b]Relative to a theoretical maximum of 33%. [c]Isotope equilibration was too rapid for accurate determination of the rate. [d]The [Na(BAr^F_{24})] was doubled. [e]Measured at -13 °C. [f]Acid was added immediately upon thawing of the reaction solution. [g]1 equiv. of $HBAr^F_{24}$ was added.

with the hypothesis that C–O activation alone controls CO_2 reduction chemistry.

We next investigated the kinetics of degenerate CO_2 exchange as a measure for the impact of LA binding on the lability of the Mo-CO_2 interaction (Scheme 3). Exposing solutions of **2-^{13}C** and a LA additive to an excess of $^{12}CO_2$ at 0 °C, resulted in decay of the resonance associated with bound CO_2 in the $^{13}C\{^1H\}$ NMR spectrum, providing a handle for kinetic analysis. The LA-free exchange rate is over two orders of magnitude faster than those of the LA-stabilized adducts. However, a systematic dependence of the exchange rates on the strength of the added LA was not observed (Table 1). The exchange rates are similar for most of the LAs, irrespective of their AN or the ^{13}C chemical shift of the adduct they form.

Scheme 3. CO_2 Self-Exchange in Mo-CO_2 LA Adducts

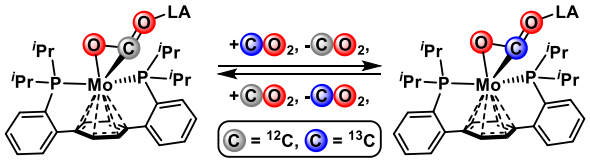

Some trends are evident from the combined kinetic data (Table 1). Borane LA adducts exchange CO_2 marginally faster in the presence of Et_2O, a competing Lewis base, supporting LA dissociation as a rate effecting step. Likewise, increasing the concentration of LA slows self-exchange, further corroborating a mechanism involving LA dissociation. For the same concentration of LA, the exchange rates are all quite similar and significantly slower than in the absence of LA. The promotion of C–O cleavage in LA adducts correlates with this kinetic factor—the 'residence time' of the CO_2 adduct, or the propensity of the substrate to remain coordinated to the metal center—not simply to the degree of CO_2

activation. Further highlighting the importance of kinetic stabilization, C–O cleavage was observed in the absence of LA when protonation was performed at low temperature (Table 1). CO_2 self-exchange likewise showed a significant dampening upon cooling, while the degree of C–O activation does not change. These data suggest that increased residence time of CO_2 at Mo, a consequence of the push-pull interaction, is instrumental for bond cleavage. A competing mechanism for protonation at Mo upon CO_2 dissociation erodes selectivity for CO_2 activation. In terms of augmenting the C–O cleavage preference, increasing the residence time is a decisive factor, independent of the mode of tuning it (temperature vs LA binding).

In summary, a labile Mo(0) CO_2 adduct interacts with a variety of LAs, increasing both the degree of activation and the kinetic stability of bound CO_2. LA addition enhances proton-induced cleavage to CO and H_2O, chemistry that correlates inversely with the kinetics of CO_2 exchange. This work establishes the residence time of a small molecule substrate in the coordination sphere of the metal as a critical factor in engendering desirable transformation chemistry of labile substrates. LAs additives are shown to improve CO_2 cleavage by *kinetic stabilization*, not simply *thermodynamic activation*.

ASSOCIATED CONTENT

Supporting Information

Detailed experimental procedures, full characterization, crystallographic details (CIF), and spectroscopic data. This material is available free of charge via the Internet at http://pubs.acs.org.

AUTHOR INFORMATION

Corresponding Author

*E-mail: agapie@caltech.edu

Notes

The authors declare no competing financial interests.

ACKNOWLEDGMENT

We thank Larry Henling and Mike Takase for invaluable crystallographic assistance T.A. is grateful for a Dreyfus fellowship and J.A.B. for a NSF graduate research fellowship. We thank the NSF (CHE-1151918 and CHE-1800501), the Dow Next Generation Education Fund, and Caltech for funding.

REFERENCES

(1) a) Liu, Q.; Wu, L.; Jackstell, R.; Beller, M. **2015**, *6*, 5933; b) Aresta, M.; Dibenedetto, A.; Angelini, A. *Chem. Rev.* **2014**, *114*, 1709; c) Appel, A. M.; Bercaw, J. E.; Bocarsly, A. B.; Dobbek, H.; DuBois, D. L.; Dupuis, M.; Ferry, J. G.; Fujita, E.; Hille, R.; Kenis, P. J. A.; Kerfeld, C. A.; Morris, R. H.; Peden, C. H. F.; Portis, A. R.; Ragsdale, S. W.; Rauchfuss, T. B.; Reek, J. N. H.; Seefeldt, L. C.; Thauer, R. K.; Waldrop, G. L. *Chem. Rev.* **2013**, *113*, 6621; d) Olah, G. A.; Prakash, G. K. S.; Goeppert, A. *J. Am. Chem. Soc.* **2011**, *133*, 12881; e) Aresta, M.; Dibenedetto, A. *Dalton Trans.* **2007**, 2975.

(2) a) Belmabkhout, Y.; Guillerm, V.; Eddaoudi, M. *Chem. Eng. J.* **2016**, *296*, 386; b) Schoedel, A.; Ji, Z.; Yaghi, O. M. *Nature Energy* **2016**, *1*, 16034; c) Leung, D. Y. C.; Caramanna, G.; Maroto-Valer, M. M. *Renew. Sust. Energ. Rev.* **2014**, *39*, 426.

(3) a) Zhang, X.; Fevre, M.; Jones, G. O.; Waymouth, R. M. *Chem. Rev.* **2018**, *118*, 839; b) Sakakura, T.; Choi, J.-C.; Yasuda, H. *Chem. Rev.* **2007**, *107*, 2365; c) Coates, G. W.; Moore, D. R. *Angew. Chem. Int. Ed.* **2004**, *43*, 6618.

(4) a) Sordakis, K.; Tang, C.; Vogt, L. K.; Junge, H.; Dyson, P. J.; Beller, M.; Laurenczy, G. *Chem. Rev.* **2018**, *118*, 372; b) Bernskoetter, W. H.; Hazari, N. *Acc. Chem. Res.* **2017**, *50*, 1049; c) Mellmann, D.; Sponholz, P.; Junge, H.; Beller, M. *Chem. Soc. Rev.* **2016**, *45*, 3954; d) Bielinski, E. A.; Lagaditis, P. O.; Zhang, Y.; Mercado, B. Q.; Würtele, C.; Bernskoetter, W. H.; Hazari, N.; Schneider, S. *J. Am. Chem. Soc.* **2014**, *136*, 10234.

(5) a) Costentin, C.; Robert, M.; Saveant, J.-M. *Chem. Soc. Rev.* **2013**, *42*, 2423; b) Benson, E. E.; Kubiak, C. P.; Sathrum, A. J.; Smieja, J. M. *Chem. Soc. Rev.* **2009**, *38*, 89; c) Rakowski Dubois, M.; Dubois, D. L. *Acc. Chem. Res.* **2009**, *42*, 1974.

(6) a) Grice, K. A. *Coord. Chem. Rev.* **2017**, *336*, 78; b) Paparo, A.; Okuda, J. *Coord. Chem. Rev.* **2017**, *334*, 136.

(7) Fesseler, J.; Jeoung, J.-H.; Dobbek, H. *Angew. Chem. Int. Ed.* **2015**, *54*, 8560.

(8) Qiao, J.; Liu, Y.; Hong, F.; Zhang, J. *Chem. Soc. Rev.* **2014**, *43*, 631.

(9) a) Forrest, S. J. K.; Clifton, J.; Fey, N.; Pringle, P. G.; Sparkes, H. A.; Wass, D. F. *Angew. Chem. Int. Ed.* **2015**, *54*, 2223; b) Jeoung, J.-H.; Dobbek, H. *Science* **2007**, *318*, 1461.

(10) a) Sampson, M. D.; Kubiak, C. P. *J. Am. Chem. Soc.* **2016**, *138*, 1386; b) Bhugun, I.; Lexa, D.; Savéant, J.-M. *J. Phys. Chem.* **1996**, *100*, 19981; c) Hammouche, M.; Lexa, D.; Momenteau, M.; Saveant, J. M. *J. Am. Chem. Soc.* **1991**, *113*, 8455.

(11) a) Takaya, J.; Iwasawa, N. *J. Am. Chem. Soc.* **2017**, *139*, 6074; b) Cammarota, R. C.; Vollmer, M. V.; Xie, J.; Ye, J.; Linehan, J. C.; Burgess, S. A.; Appel, A. M.; Gagliardi, L.; Lu, C. C. *J. Am. Chem. Soc.* **2017**, *139*, 14244; c) Devillard, M.; Declercq, R.; Nicolas, E.; Ehlers, A. W.; Backs, J.; Saffon-Merceron, N.; Bouhadir, G.; Slootweg, J. C.; Uhl, W.; Bourissou, D. *J. Am. Chem. Soc.* **2016**, *138*, 4917.

(12) a) Bagherzadeh, S.; Mankad, N. P. *J. Am. Chem. Soc.* **2015**, *137*, 10898; b) Krogman, J. P.; Foxman, B. M.; Thomas, C. M. *J. Am. Chem. Soc.* **2011**, *133*, 14582.

(13) a) Yoo, C.; Lee, Y. *Chem. Sci.* **2017**, *8*, 600; b) Rauch, M.; Parkin, G. *J. Am. Chem. Soc.* **2017**, *139*, 18162; c) Kim, Y.-E.; Kim, J.; Lee, Y. *Chem. Commun.* **2014**, *50*, 11458; d) Jiang, Y.; Blacque, O.; Fox, T.; Berke, H. *J. Am. Chem. Soc.* **2013**, *135*, 7751.

(14) a) Jin, G.; Werncke, C. G.; Escudié, Y.; Sabo-Etienne, S.; Bontemps, S. *J. Am. Chem. Soc.* **2015**, *137*, 9563; b) Chakraborty, S.; Zhang, J.; Krause, J. A.; Guan, H. *J. Am. Chem. Soc.* **2010**, *132*, 8872; c) Laitar, D. S.; Müller, P.; Sadighi, J. P. *J. Am. Chem. Soc.* **2005**, *127*, 17196.

(15) Mo complexes have been employed previously for CO_2 reduction chemistry. For select examples, see: a) Zhang, Y.; Williard, P. G.; Bernskoetter, W. H. *Organometallics* **2016**, *35*, 860; b) Neary, M. C.; Parkin, G. *Chem. Sci.* **2015**, *6*, 1859; c) Clark, M. L.; Grice, K. A.; Moore, C. E.; Rheingold, A. L.; Kubiak, C. P. *Chem. Sci.* **2014**, *5*, 1894.

(16) a) Carden, R. G.; Ohane, J. J.; Pike, R. D.; Graham, P. M. *Organometallics* **2013**, *32*, 2505; b) Bernskoetter, W. H.; Tyler, B. T. *Organometallics* **2011**, *30*, 520; c) Contreras, L.; Paneque, M.; Sellin, M.; Carmona, E.; Perez, P. J.; Gutierrez-Puebla, E.; Monge, A.; Ruiz, C. *New J. Chem.* **2005**, *29*, 109; d) Alvarez, R.; Carmona, E.; Marin, J. M.; Poveda, M. L.; Gutierrez-Puebla, E.; Monge, A. *J. Am. Chem. Soc.* **1986**, *108*, 2286.

(17) Gambarotta, S.; Floriani, C.; Chiesi-Villa, A.; Guastini, C. *J. Am. Chem. Soc.* **1985**, *107*, 2985.

(18) a) Seravalli, J.; Ragsdale, S. W. *Biochemistry* **2008**, *47*, 6770; b) We could not find a reported T_1 time for N_2 gas in organic solvent. There are, however, extensive studies on ^{15}N relaxation parameters at low temperature in liquid N_2. See Ishol, L.M.; Scott, T.A.; Goldblatt, M. *J. Mag. Res.* **1976**, *23*, 313.

(19) Ishol, L. M.; Scott, T. A.; Goldblatt, M. *J. Mag. Res.* **1976**, *23*, 313.

(20) Buss, J. A.; Edouard, G. A.; Cheng, C.; Shi, J.; Agapie, T. *J. Am. Chem. Soc.* **2014**, *136*, 11272.

(21) Schneider, J.; Jia, H.; Muckerman, J. T.; Fujita, E. *Chem. Soc. Rev.* **2012**, *41*, 2036.

(22) a) Chapovetsky, A.; Do, T. H.; Haiges, R.; Takase, M. K.; Marinescu, S. C. *J. Am. Chem. Soc.* **2016**, *138*, 5765; b) Sampson, M. D.; Nguyen, A. D.; Grice, K. A.; Moore, C. E.; Rheingold, A. L.; Kubiak, C. P. *J. Am. Chem. Soc.* **2014**, *136*, 5460; c) Bhugun, I.; Lexa, D.; Savéant, J.-M. *J. Am. Chem. Soc.* **1996**, *118*, 1769; d) DuBois, D. L.; Miedaner, A.; Haltiwanger, R. C. *J. Am. Chem. Soc.* **1991**, *113*, 8753; e) Ishida, H.; Tanaka, K.; Tanaka, T. *Organometallics* **1987**, *6*, 181.

(23) a) Sahoo, D.; Yoo, C.; Lee, Y. *J. Am. Chem. Soc.* **2018**, *140*, 2179; b) Tsai, J. C.; Khan, M.; Nicholas, K. M. *Organometallics* **1989**, *8*, 2967.

(24) Vol'pin, M. E. K., I.S. *Pure Appl. Chem.* **1973**, *33*, 567.

(25) a) Geri, J. B.; Shanahan, J. P.; Szymczak, N. K. *J. Am. Chem. Soc.* **2017**, *139*, 5952; b) Simonneau, A.; Turrel, R.; Vendier, L.; Etienne, M. *Angew. Chem. Int. Ed.* **2017**, *56*, 12268.

(26) The N1–N2 distance elongates by 0.06 Å and the N2–B distance, at 1.586(5) Å, is similar to that of a reported borane N_2 adduct (see ref 25a).

(27) a) Parks, D. J.; Piers, W. E.; Yap, G. P. A. *Organometallics* **1998**, *17*, 5492; b) Horton, A. D.; de With, J. *Organometallics* **1997**, *16*, 5424.

(28) Lewiński, J.; Kubicki, D. In *Encyclopedia of Spectroscopy and Spectrometry (Third Edition)*; Tranter, G. E., Koppenaal, D. W., Eds.; Academic Press: Oxford, 2017, p 318.

(29) Cation **6** is accessible via addition of $HBAr^{F}_{24}$ to a Mo(0) monocarbonyl complex (Scheme S1).

(30) Xu, T.; Chen, E. Y. X. *J. Am. Chem. Soc.* **2014**, *136*, 1774.

(31) Bergquist, C.; Bridgewater, B. M.; Harlan, C. J.; Norton, J. R.; Friesner, R. A.; Parkin, G. *J. Am. Chem. Soc.* **2000**, *122*, 10581.

(32) Beckett, M. A.; Strickland, G. C.; Holland, J. R.; Sukumar Varma, K. *Polymer* **1996**, *37*, 4629.

(33) Even with isotopic enrichment, the C–O stretches of the alkali metal LA adducts were inadequately resolved to be assigned with confidence. This limits the available IR data to three points; however, a clear linear trend is observed for both the ^{12}C and ^{13}C isotoplogues.

(34) These reactions were performed with strict exclusion of N_2 to avoid potential exchange prior to protonation.

(35) The theoretical maximum of which is 33% (*vide supra*).

(36) Protonation experiments were performed in a 2 PhCl : 1 Et_2O solvent mixture, which solubilizes both alkali metal and borane LAs and their adducts.

For Table of Contents Only

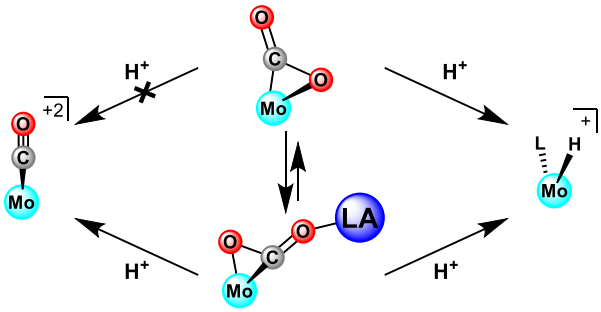

Thermodynamic activation *and* Kinetic stabilization